

Arunika H. L. A. N. Gunawardena · Kathy Sault
Petra Donnelly · John S. Greenwood
Nancy G. Dengler

Programmed cell death and leaf morphogenesis in *Monstera obliqua* (Araceae)

Received: 12 January 2005 / Accepted: 11 March 2005 / Published online: 2 June 2005
© Springer-Verlag 2005

Abstract The unusual perforations in the leaf blades of *Monstera obliqua* (Araceae) arise through programmed cell death early in leaf development. At each perforation site, a discrete subpopulation of cells undergoes programmed cell death simultaneously, while neighboring protoderm and ground meristem cells are unaffected. Nuclei of cells within the perforation site become terminal deoxynucleotidyl transferase-mediated dUTP nick end labeling (TUNEL)-positive, indicating that DNA cleavage is an early event. Gel electrophoresis indicates that DNA cleavage is random and does not result in bands that represent multiples of internucleosomal units. Ultrastructural analysis of cells at the same stage reveals misshapen, densely stained nuclei with condensed chromatin, disrupted vacuoles, and condensed cytoplasm. Cell walls within the perforation site remain intact, although a small disk of dying tissue becomes detached from neighboring healthy tissues as the leaf expands and stretches the minute perforation. Exposed ground meristem cells at the rim of the perforation differentiate as epidermal cells. The cell biology of perforation formation in *Monstera* resembles that in the aquatic plant *Aponogeton madagascariensis* (Aponogetonaceae; Gunawardena et al. 2004), but the absence of cell wall degradation and the simultaneous execution of programmed cell death throughout the perforation site reflect the convergent evolution of this distinct mode of leaf morphogenesis in these distantly related plants.

Keywords Leaf development · *Monstera* · Perforation formation · Programmed cell death · TUNEL assay · Ultrastructure

Abbreviations PCD: Programmed cell death · TUNEL: Terminal deoxynucleotidyl transferase-mediated dUTP nick end labeling

Introduction

The leaves of many *Monstera* species are highly unusual in that the blades are perforated by conspicuous holes. In some species, a series of large, regularly spaced perforations extend from the midrib to the leaf margin and may break through the leaf edge, forming pinnately dissected or pinnatifid leaves. In other species, perforations are restricted to the blade near the midrib and the margin of the leaf remains entire (Madison 1977). Fenestrate leaves are also reported from five related genera of the Araceae (Mayo et al. 1997, 1998) and from a single species of the only distantly related Aponogetonaceae (*Aponogeton madagascariensis*; Sergueeff 1907; Gunawardena et al. 2004). The function(s) of perforations in *Monstera* and other aroids are unknown, but it is likely that they serve to reduce effective leaf size and thus heat transfer properties, much like the individual leaflets of more conventional compound leaves (Madison 1977). Another intriguing hypothesis is that perforations serve as camouflage by disrupting the leaf outline or as signals to herbivores that induced chemical and/or physical defenses may already be present (Brown and Lawton 1991).

Despite the rarity of this phenomenon, botanists have long been fascinated with the mode of origin of leaf perforations in aroids. Trecul (1854) recognized that the perforations arose through a process that was completely different from the developmental mechanisms that give rise to leaves of complex shape in other plants. He observed that developing leaves first form a simple, continuous leaf blade and then only later do tissues at the perforation sites become discolored and “destroy themselves”, forming the perforations. Schwartz (1878) described the large, elaborately perforate leaves of

A. H. L. A. N. Gunawardena · K. Sault
P. Donnelly · N. G. Dengler (✉)
Department of Botany, University of Toronto,
Toronto, ON, M5S 1A1, Canada
E-mail: dengler@botany.utoronto.ca
Fax: +1-416-9785878

J. S. Greenwood
Department of Botany, University of Guelph,
Guelph, ON, N1G 2W1, Canada

Monstera deliciosa and suggested that the death of tissues within the perforation site exposed internal leaf tissues that would then form a secondary epidermis in continuity with the original primary epidermis. Melville and Wrigley (1969) dissected shoot tips of *M. deliciosa* and described the appearance of the “necrotic areas” on the developing leaf blades. In mature leaves, the sizes of individual perforations were thought to reflect their time of origin and the distribution of expansion growth between margin and midrib (Melville and Wrigley 1969). Kaplan (1984) illustrated perforation formation in *M. deliciosa* with scanning electron micrographs but, other than describing the process of perforation formation as “necrosis”, no author has yet characterized the internal cellular processes associated with cell death in *Monstera*.

Programmed cell death (PCD) is usually regarded as a genetically encoded cell death that performs a detectable function in the life of the plant (Barlow 1982; Morgan and Drew 2004). Developmentally regulated PCD, such as tracheary element differentiation or deletion of the embryonic suspensor, occurs at a predictable time and place and is induced by endogenous factors. Environmentally induced PCD, such as the hypersensitive response to pathogens or the development of lysigenous aerenchyma triggered by hypoxia, is initiated by biotic or abiotic exogenous signals. In contrast, necrotic cell death results from accidental or random injury such as exposure to toxins or a lethal temperature and affects only tissues exposed to these acute exogenous factors (Morgan and Drew 2004; Nooden 2004). The species specificity and predictability of perforation location in the leaves of *Monstera* suggest that perforations arise from developmentally regulated PCD rather than necrosis and, indeed, several recent reviews of PCD in plants cite the perforate leaves of *Monstera* species as examples of developmentally regulated PCD (Greenberg 1996; Jones and Dangel 1996; Beers 1997; Pennell and Lamb 1997; Dangel et al. 2000; Huelskamp and Schnittger 2004).

Even in animal systems, where PCD is well-characterized, it is clear that cell death takes diverse forms (Nooden 2004; Lockshin 2004). At least three cytologically distinct forms of PCD occur (apoptotic, lysosomal/autophagic, and nonlysosomal vesiculate), and each may have many variants (Clarke 1990). During apoptosis, condensation of the nucleus, chromatin and cytoplasm is prominent and the cell membrane becomes convoluted and forms blebs. In autophagic degeneration, numerous autophagic vesicles form and engulf organelles, while in nonlysosomal PCD, general disintegration occurs without vacuole formation, at least at early stages of cell death. Apoptotic PCD typically involves the cleavage of DNA into internucleosomal fragments. DNA fragmentation is characterized in situ by the TUNEL assay (terminal deoxynucleotidyl transferase-mediated dUTP nick end labeling) and by gel electrophoresis where multiples of the 180 bp internucleosomal units form a ladder-like pattern. Many forms of plant PCD express the hallmarks of animal apoptosis and other kinds of animal PCD, including nuclear condensation, formation of lytic

vesicles, and cleavage of DNA into internucleosomal units (Dangel et al. 2000; Jones 2001; Hoeberichts and Woltering 2002; Nooden 2004). In plant cells, the presence of a cell wall precludes removal of the dying protoplast by neighboring cells, although the cell wall is degraded in certain forms of plant PCD (Jones 2001; Obara and Fukuda 2004). For instance, formation of lysigenous aerenchyma in maize roots in response to hypoxia resembles both apoptotic and lysosomal PCD: nuclei become TUNEL-positive, DNA is cleaved into internucleosomal units, organelles become surrounded by (presumably) lytic vesicles, and the cell wall chemistry is altered before complete degradation (Gunawardena et al. 2001a, 2001b; Evans 2003). In contrast, the well-characterized process of tracheary element differentiation is unlike any of the forms of animal PCD: the vacuole first releases sequestered proteases and nucleases, rapidly acidifying the cytoplasm and resulting in the degradation of nuclear and chloroplastic DNA without detectable laddering (Groover et al. 1997; Obara et al. 2001; Ito and Fukuda 2002; Obara and Fukuda 2004). Prominent chromatin condensation does not occur, but organelles swell, and first their matrices and then their membranes disintegrate. The primary cell wall is degraded at specific locations to form the perforation that joins individual tracheary elements into a vessel (Nakashima et al. 2000).

Morphogenesis of the unusual perforate leaves of *Monstera* species has been hypothesized to incorporate many of these common hallmarks of plant PCD as has been shown for the lace plant, *Aponogeton madagascariensis* (Gunawardena et al. 2004). Lace plant grows as a submerged aquatic, and perforation formation occurs in a predictable pattern that reflects the grid-like arrangement of longitudinal and cross veins. PCD is initiated in centrally located cells within each interveinal panel, but later extends to more peripheral cells, stopping ~5 cell layers from the vascular tissue. PCD is first expressed by an alteration of cytoplasmic streaming and a loss of anthocyanin coloration, reflecting the rupture of the tonoplast and acidification of the cytoplasm (Gunawardena et al. 2004). Nuclei become TUNEL-positive at the same time, but laddering was not detected by gel electrophoresis, indicating that DNA cleavage is random. These changes are followed by shrinkage of the cytoplasm and the late degradation of organelles. Degradation of the cell walls results in formation of a narrow perforation, which enlarges as the leaf expands. While the time and place of perforation formation in lace plant facilitates the cytological study of PCD, this is not the case for *Monstera* species. Perforation development occurs early, when the young leaf is tightly enclosed by two to three older leaves (Melville and Wrigley 1969; Kaplan 1984), and cannot be readily observed in living material. Nevertheless, our goal was to characterize this remarkable case of developmental convergence by examining aspects of the cell biology of perforation formation in the leaves of *Monstera* and to compare the specific steps in the execution of cell death to those in the more tractable lace plant.

Materials and methods

Plant material

Swiss cheese plant (*Monstera obliqua*) was supplied from Humber Nurseries (Toronto, ON, Canada), and plant material was maintained at 20°C and ca. 300 $\mu\text{mol m}^{-2} \text{s}^{-1}$ light in greenhouses at the University of Toronto. Growing shoots display a heteroblastic series in which first a prophyll and then small, imperforate leaves are formed. Therefore, material for further study was selected only from adult-phase shoots that had already begun to form large perforate leaves. Mature leaves and shoot tips were dissected and tissue allocated to one of five arbitrarily defined stages of perforation development (stage 1—pre-perforation; stage 2—programmed cell death in discrete disk of tissue at perforation site; stage 3—detachment of tissue disk from surrounding expanding tissues to form perforation; stage 4—leaf expansion; stage 5—maturity). These stages of tissue development were selected to facilitate comparison of cells across different techniques, as leaf plastochron ages are not finely graded enough to distinguish the key stages of perforation formation.

Light microscopy

Shoot tips were fixed in FAA (formalin: acetic acid: 70% ethanol; 1:1:18, by vol.) overnight and rinsed in 70% ethanol. Large samples were dehydrated through a graded tertiary butyl alcohol series and embedded in Paraplast. Serial sections (5- μm thick) of four shoot tips (> 5-cm long) were obtained using a Reichert Histostat rotary microtome (Reichert Scientific Instruments, New York, USA) and stained with 0.05% aqueous toluidine blue. Smaller specimens were dehydrated in an ethanol series, infiltrated with an acetone : Spurr resin mixture, and embedded in Spurr resin. Serial sections (2- μm thick) of five stage 1 and six stage 2 leaves were made using a RMC MT-7 ultramicrotome and stained in 0.05% toluidine blue in 0.01% NaCO_3 . Serial sections were examined under brightfield optics using a Reichert-Jung Polyvar (Vienna, Austria) microscope and images recorded using a Nikon DXM 1200 digital camera (Nikon Canada, Mississauga, Canada).

Scanning electron microscopy

Tissue samples were fixed in FAA (formalin: acetic acid: 70% ethanol; 1:1:18, by vol.) for overnight. Samples were dehydrated through a graded ethanol series and dried using a Tousimis Autosamdri-814 critical point dryer (Tousimis Research Corporation, Rockville, MD, USA). The samples were then mounted on stubs, coated with gold on a Cressington 108 sputter-coater (Cressington Scientific Instruments, Cramberry Township,

PA, USA.), and observed using a Hitachi S-2500 scanning electron microscope (Tokyo, Japan). Images were recorded using a Quartz PCI version 5.1 camera (Quartz Imaging Corporation, Vancouver, Canada).

Transmission electron microscopy

Tissue samples were fixed overnight in 2% glutaraldehyde in 0.05 M sodium cacodylate buffer (pH 6.9), washed in the same buffer, then postfixed in 2.5% aqueous osmium tetroxide for 2 h at room temperature. Tissues were dehydrated in a graded ethanol series, infiltrated through ethanol:Spurr resin mixtures, embedded in pure Spurr resin and polymerized at 70°C for 9 h. Gold sections were cut on a Reichert-Jung ultramicrotome (Vienna, Austria), collected onto formvar-coated grids, and stained with uranyl acetate and lead citrate. Observations were made using a

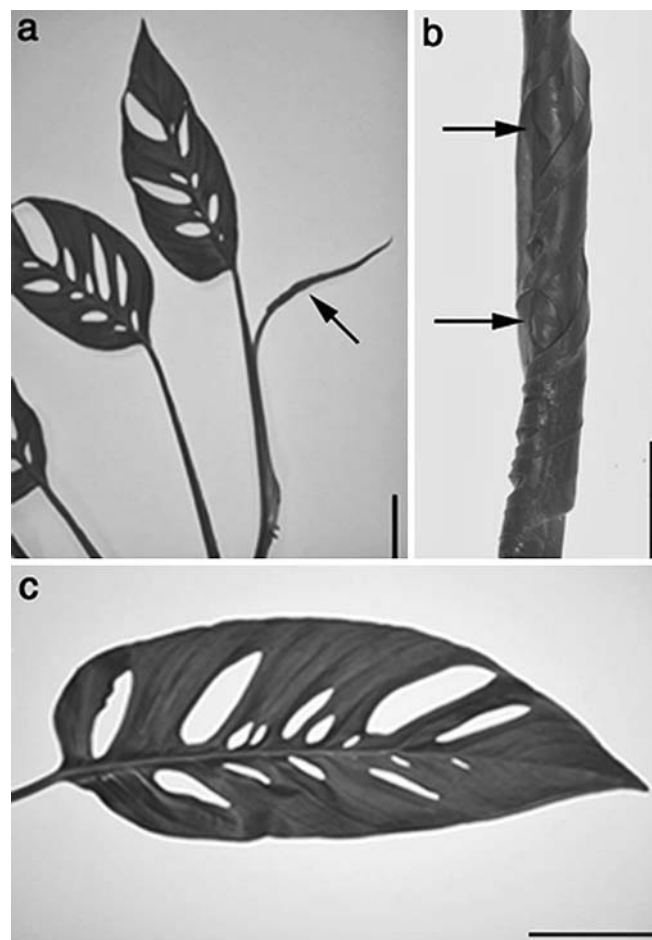
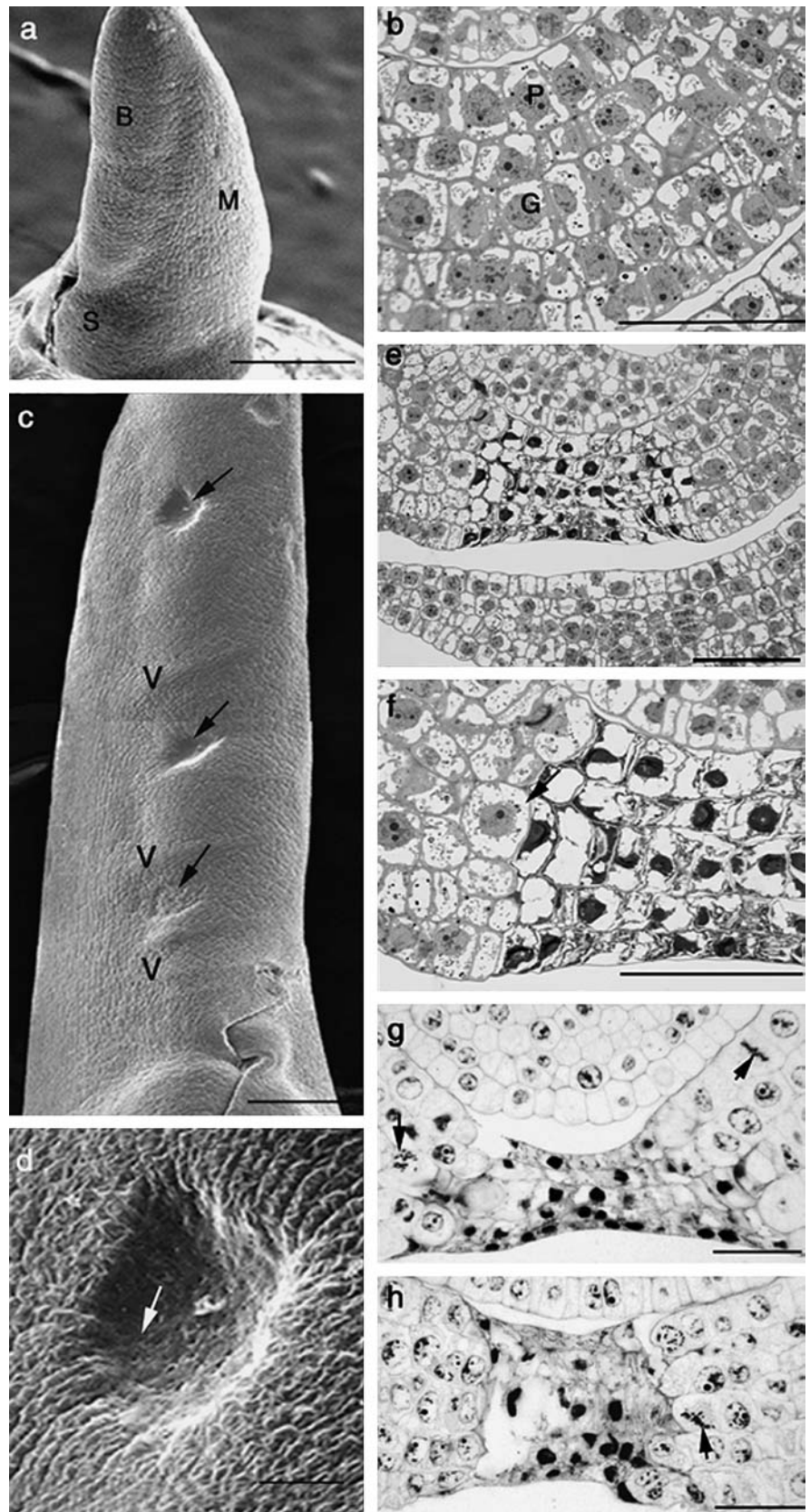


Fig. 1 Mature and expanding leaves of *Monstera obliqua* **a** Whole shoot showing young leaf (arrow) expanding from sheath of next oldest leaf. **b** Convolutely rolled leaf blade showing presence of perforations (arrows) prior to unfurling from apical bud. **c** Mature leaf showing distribution of perforations on broad and narrow lamina halves. Scale bars = 3 cm

Phillips 201 transmission electron microscope (Eindhoven, Netherlands) and recorded digitally using an AMT

CCD camera system (Advanced Microscopy Techniques, Danvers, USA).

Fig. 2 Developing leaves of *Monstera obliqua*. **a, b** Early plastochron 2 leaf at stage 1 (preperforation) of tissue development. **c–h** Early plastochron 3 leaf at stage 2 (perforation initiation) of tissue development. **a** Scanning electron micrograph of stage 1 leaf, showing thickened midrib, convolutedly rolled blade, and sheathing leaf base. **b** Cross section of tissue from interveinal area prior to perforation formation (stage 1). **c** Scanning electron micrograph of stage 2 leaf showing simultaneous initiation of three perforations (*arrows*) and placement of secondary lateral veins. **d** Higher magnification of perforation site near leaf apex showing sunken appearance of dying cells (*arrow*). **e** Cross section of stage 2 perforation site showing uniform appearance of cells in each tissue layer across the diameter of the perforation, indicating simultaneous PCD. **f** Higher magnification of same site. Note sharp boundary (*arrow*) between dying cells of perforation (*right*) and healthy cells at periphery (*left*). **g** Late stage 2 perforation showing mitotic figures (*arrows*) in neighboring ground and dermal cells. **h** Late stage 2 perforation showing mitotic figure (*arrow*) directly adjacent to dying cells. *B*, blade; *G*, ground meristem; *M*, midrib; *P*, protoderm; *S*, sheath; *V*, vein. Scale bars = 0.3 mm for **a, c**; 50 μ m for **b, d–h**

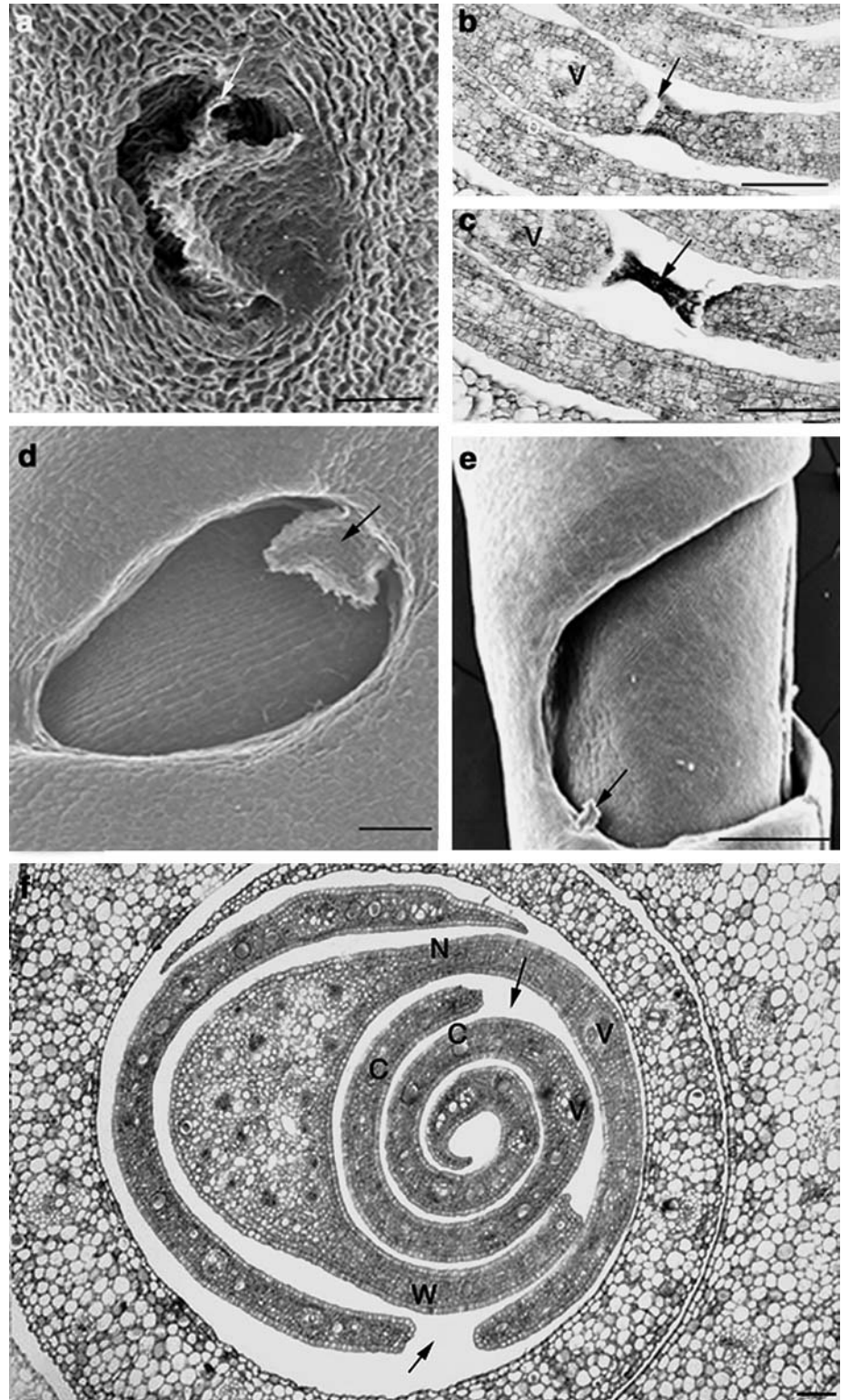


Terminal deoxynucleotidyl transferase-mediated dUTP nick end labeling (TUNEL) assay

Tissue samples were fixed in FAA for overnight and washed in 70% ethanol. The TUNEL assay was carried

out according to the manufacturer's (Roche Diagnostics GmbH, Mannheim, Germany) instructions, and nuclei were stained by incubating in 3% (w/v) propidium iodide for 2 min. Samples were observed with a Zeiss LSM 410 inverted confocal laser scanning microscope (Carl

Fig. 3 Developing leaves of *Monstera obliqua*. a-c Stage 3 (detachment of tissue disk from surrounding expanding tissue to form perforation) in late plastochron 3 of leaf development. d-f Stage 4 (leaf expansion) in plastochron 4 to 6 leaves. **a** Scanning electron micrograph showing detachment (*arrow*) of disk of dying tissue at boundary of perforation site. **b** Cross section of early stage 3 perforation site (*arrow*). Note differentiation of vascular tissue in veins. **c** Cross section of late stage 3 perforation site (*arrow*). **d** Scanning electron micrograph of early stage 4 perforation showing detached disk of dying tissue (*arrow*). **e** Scanning electron micrograph of late stage 4 perforation showing detached disk of dying tissue (*arrow*). **f** Cross section of early stage 4 leaf showing convolutedly rolled blade within sheath of next older leaf. Note perforations (*arrows*) in narrow blade half (rolled to the outside) and in wide blade (half rolled to the inside). Compare with Fig. 1a, c. Note differentiation of vascular tissues in veins and raphide crystal idioblasts in ground tissue. C, raphide crystal idioblast; N, narrow blade half; W, wide blade half; V, vein. Scale bars = 50 μ m for a-d, f; 0.5 mm for e



Zeiss Canada Ltd., Toronto, Canada) with a filter configuration of excitation—488 nm, emission—515 nm for fluorescein isothiocyanate and excitation—543 nm, emission—570 nm for propidium iodide. A negative control was carried out without TdT enzyme and a positive control was carried out with DNase1. Experiments were repeated three times.

DNA isolation and electrophoresis

Genomic DNA was isolated from stages 1 to 5. About 25–50 mg of leaf tissue for each treatment was frozen in liquid nitrogen immediately after sampling and ground with a mortar and pestle to a fine powder. Isolation of DNA was carried out using a DNeasy Plant Mini Kit

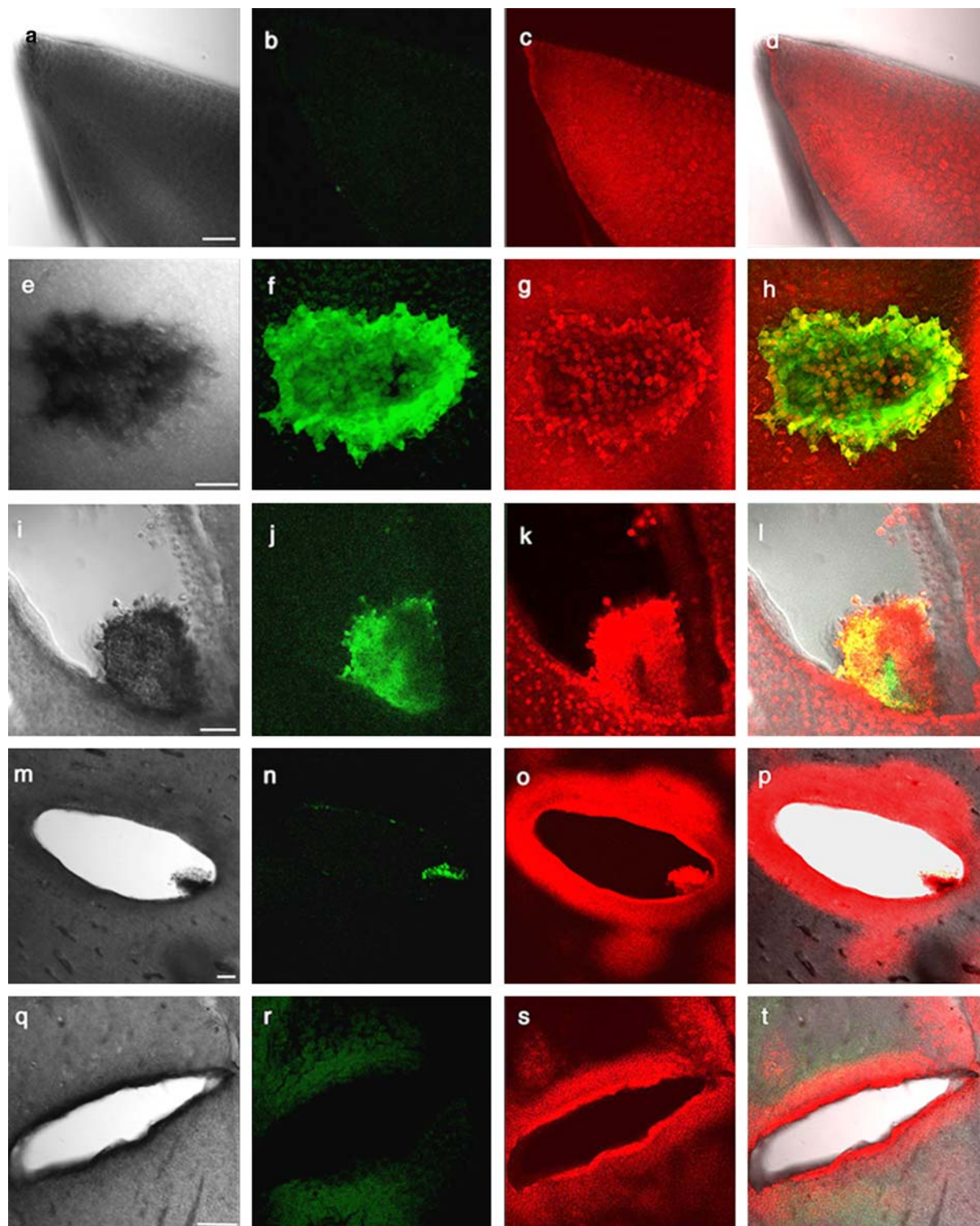


Fig. 4 Confocal microscopy (CM) and differential interference contrast (DIC) microscopy showing detection of DNA cleavage by TUNEL assay in leaves of *Monstera obliqua*. **a–d** stage 1. **a** DIC image of leaf blade. **b** CM image showing absence of TUNEL-positive nuclei. **c** CM image of propidium iodide-stained nuclei. **d** Merged image of a–c. **e–h** stage 2. **e** DIC image of perforation site. **f** CM image showing TUNEL-positive nuclei in cells of perforation site. **g** CM image showing propidium iodide-stained nuclei. **h** Merged image of e–g. **i–l** early stage 4. **i** DIC image of perforation showing detached disk of dead tissue and rim of expanding perforation. **j** CM image showing TUNEL-positive nuclei in disk of detached tissue. **g** CM image showing propidium iodide-stained nuclei. **h** Merged image of e–g. **m–p** Late stage 4. **m** DIC image of perforation. **n** CM image showing some TUNEL-positive nuclei in disk of dead tissue. **o** CM image showing propidium iodide-stained nuclei. **p** Merged image of m–o. **q–t** stage 5. **q** DIC image of perforation. **r** CM image showing absence of TUNEL-positive nuclei. **s** CM image showing propidium iodide-stained nuclei. **t** Merged image of q–s. Scale bars = 50 μm

(QIAGEN, Mississauga, Canada) according to the manufacturer's instructions. To observe DNA fragmentation, samples (0.5 μg per lane) were run on a 1.0% agarose gel with 0.5 $\mu\text{g ml}^{-1}$ (final concentration) ethidium bromide at constant 50 V using a 100-bp ladder. Gels were photographed using a Digi Doc IT System (Ultraviolet Products Limited, Cambridge, UK).

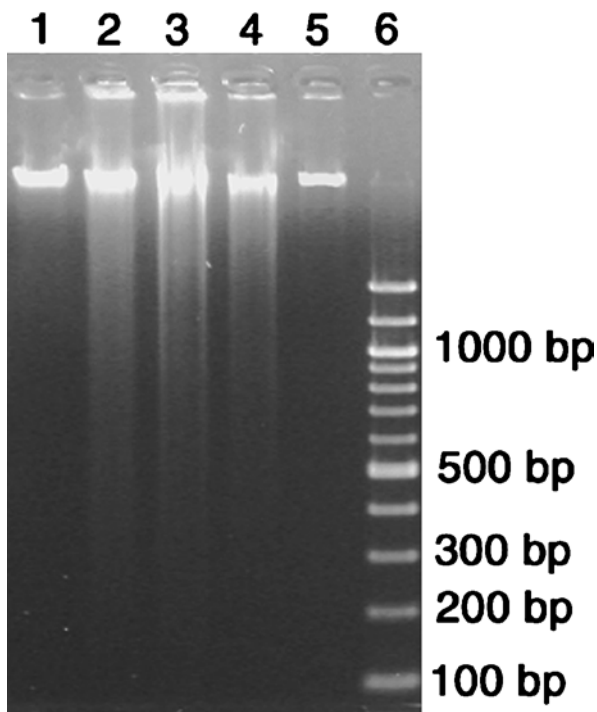


Fig. 5 Agarose gel of DNA extracted from leaves of *Monstera obliqua* lane 1, stage 1 (preperforation tissue); lane 2, stage 2 (perforation initiation); lane 3, stage 3 (detachment of disk of dying cells); lane 4, stage 4 (leaf expansion); lane 5, stage 5 (mature leaves); lane 6, 100-bp ladder

Results

Leaf morphogenesis

Adult leaves of *Monstera obliqua* have sheathing bases, narrow elongate petioles and broad blades with conspicuous elliptical perforations that are positioned between the lateral veins (Fig. 1a, c). Typically, three to four large perforations that extend from near the midrib to the margin are formed in each half of the lamina, and a variable number of medium and small sized perforations are present closer to the midrib. The leaf blade is asymmetrical, with more numerous and larger perforations formed within the wider half. Leaf arrangement is distichous, and the position of the narrow, outer blade half alternates between successive leaves, lending dorsiventral symmetry to the whole shoot (Fig. 1a). Leaf blades reach almost full expansion while still rolled in the apical bud; during the final stages of development, the petiole elongates, pushing the blades out from the sheathing base of the next older leaf and revealing the preformed perforations (Fig. 1a, b).

Perforations are not detectable structurally until late plastochron 2 of leaf development. Early plastochron 2 leaves, having a distal convolutedly folded blade with a thickened midrib region and a proximal sheathing base that encircles the shoot apical meristem, are designated as stage 1 (preperforation) tissue (Fig. 2a). During stage 1, the protoderm and ground meristem tissue layers between the lateral vein procambial strands are uniform in appearance: cells have large, rounded nuclei and multiple large vacuoles (Fig. 2b).

Perforations are first apparent in leaves that are in late plastochron 2 or early plastochron 3 of leaf development (stage 2, perforation initiation). Analysis of serial sections indicates that individual perforations appear simultaneously throughout the leaf blade, although only a few are visible on the abaxial side of an intact leaf due to the convolute rolling of the blade (Fig. 2c). Perforations arise equidistantly between externally visible secondary vein ribs (Fig. 2c) and before the formation of tertiary and higher order vein procambial strands within the developing blade. Stage 2 perforations are variable in diameter (range 50–200 μm , mean $135.3 \pm 10.6 \mu\text{m}$) and in number of cells across (range 7–20, mean 13.5 ± 1.1), foreshadowing variation in mature size. The dying cells are shrunken in contrast to neighboring healthy cells, so that developing perforations can be identified as sunken depressions on the abaxial surface of the leaf (Fig. 2c, d). Cells in all tissue layers appear to initiate PCD simultaneously (Fig. 2e–h). The sharp boundary between dying and healthy cells is striking, with plump, turgid cells adjacent to shrunken dying ones (Fig. 2f). Cell death appears to occur rapidly, as intermediate stages in the death process were rarely observed. Mitotic figures are frequent at this stage,

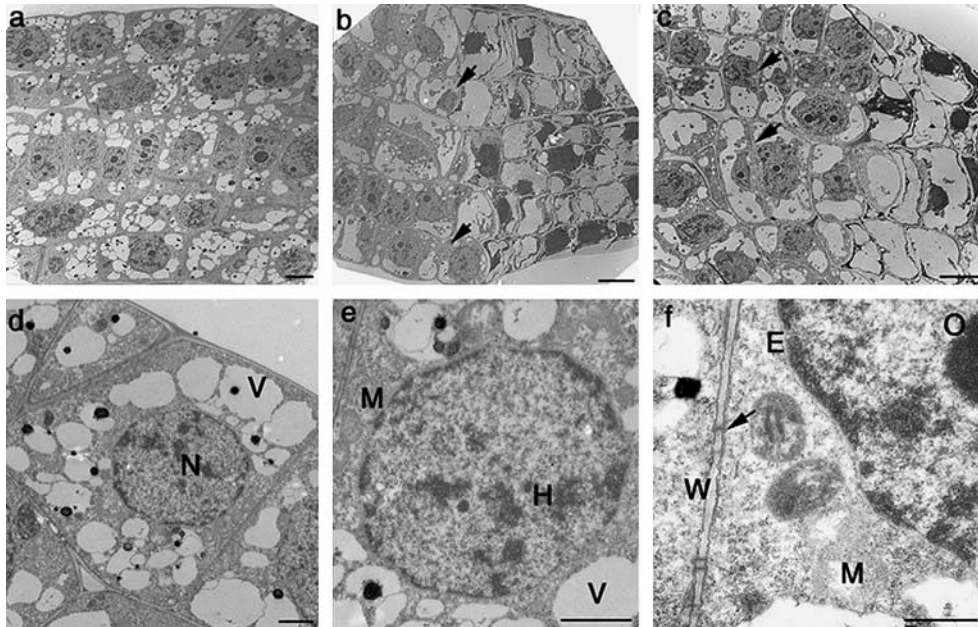


Fig. 6 Transmission electron micrographs of developing leaves of *Monstera obliqua*. **a** Low magnification image of stage 1 tissue prior to perforation formation. Note rounded nuclei, numerous vacuoles and dense cytoplasm. **b** Low magnification image of stage 2 tissue at boundary between dying cells of perforation site (*right*) and living cells at periphery (*left*). Note round, multinucleolate nuclei, enlarged vacuoles and convex shape of living cells at boundary (*arrows*). In contrast adjacent dying cells have irregular, densely stained nuclei, large clear regions, and densely stained peripheral cytoplasm. **c** Low magnification image of stage 2 tissue at periphery of perforation. Note regular cell shape and thin cell walls indicating recent cell divisions (*arrows*). **d–f** Higher magnification of stage 1 cells. **d** Dermal cell showing nucleus, vacuoles and uniform cytoplasm. **e** Nucleus of ground cell showing heterochromatin, nucleoli and intact nuclear envelope. **f** Cytoplasm of ground cell showing nuclear envelope, mitochondria, and thin cell wall with plasmodesmata (*arrow*). *E*, nuclear envelope; *H*, heterochromatin; *M*, mitochondrion; *N*, nucleus; *O*, nucleolus; *V*, vacuole, *W*, wall. Scale bars = 10 μm for a–c; 2 μm for d–f

including cells directly adjacent to perforation sites (Fig. 2 g–h).

As the leaf blade expands in late plastochron 3, the disk-shaped zone of dying cells becomes detached from surrounding tissue along most of its circumference, forming the nascent perforation (stage 3; Fig. 3a–c). This detachment exposes the anticlinal walls of dermal and ground tissues to the external surface of the leaf. After detachment, cells within the perforation site are completely collapsed, with densely stained cell walls and protoplasts (Fig. 3c). Continued expansion of the rolled leaf blade during subsequent plastochrons is accompanied by an increase in perforation size, with the shrunken disk of dead tissue adhering to the margin (stage 4; Fig. 3 d, e). At this stage, expanding leaves are fully enclosed by the sheathing base of the next oldest leaf (Fig. 3f). In each leaf, the narrow blade half with smaller perforations is rolled to the outside, while the wider blade half with larger perforations is rolled to the inside (Fig. 3f).

DNA cleavage during perforation formation

Nuclear DNA degradation during perforation formation was characterized using the TUNEL assay on whole mounts of fixed leaves. In stage 1 leaves, nuclei of all visible cells stain with propidium iodide, but TUNEL-positive nuclei are absent (Fig. 4 a–d). In early stage 2 leaves, TUNEL-positive nuclei are present throughout the perforation zone of dying cells, in sharp contrast to adjacent cells which are TUNEL-negative (Fig. 4e–h). The fluorescein label revealing cleaved DNA clearly co-localizes with the propidium iodide-stained nuclei (Fig. 4h). During stage 3, nuclei within the disk of detached tissue remain TUNEL-positive, while nuclei of adjacent tissues and tissues on the rim of the expanding perforation are TUNEL-negative (Fig. 4i–l). Some nuclei within the disk continue to be TUNEL-positive, even during relatively late stages of blade expansion (stage 4, Fig. 4m–p), but in fully expanded leaves (stage 5), all cells are TUNEL negative (Fig. 4q–t).

Genomic DNA was isolated from all five stages and separated by agarose gel electrophoresis (Fig. 5). DNA cleavage was indicated by a conspicuous uniform smear of DNA at stages 2 (lane 2), 3 (lane 3) and 4 (lane 4), but was absent when DNA was isolated from pre-perforation stage 1 leaves (lane 1) or from mature stage 5 leaves (lane 5). A laddering pattern, formed by multiples of internucleosomal units of ~ 180 bp, was not observed at any stage. Consistent results were obtained in three independent DNA extractions.

Cellular ultrastructure during PCD

At stage 1, protoderm and ground meristem cells are polygonal in shape, with centrally positioned, round

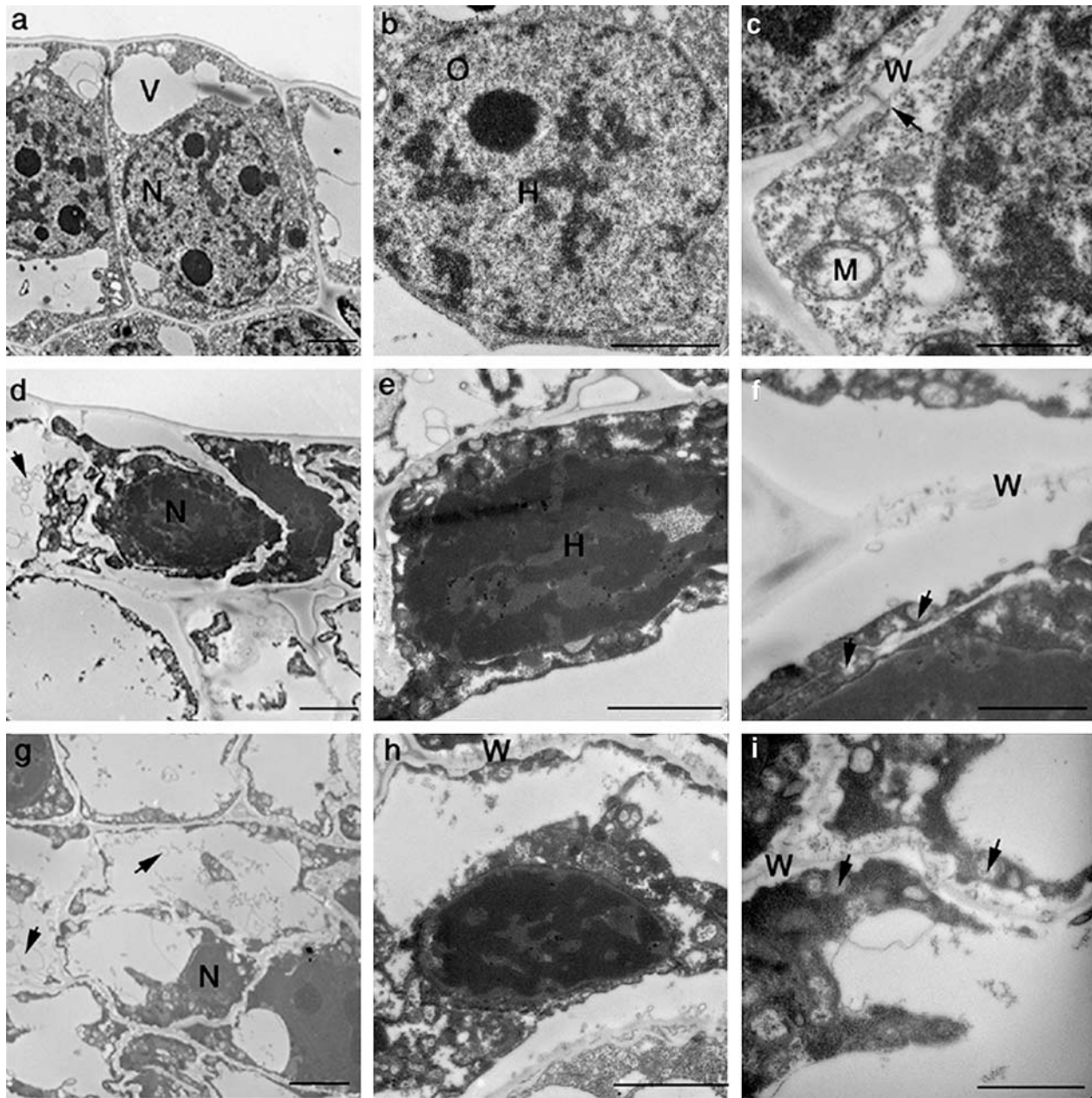


Fig. 7 Transmission electron micrographs of stage 2 perforation sites in developing leaves of *Monstera obliqua*. **a–c** Living cells adjacent to perforation site. **a** Dermal cell with rounded nucleus, coalescing vacuoles and uniform cytoplasm. **b** Nucleus showing heterochromatin, nucleoli and diffuse nucleoplasm. **c** Cytoplasm with mitochondria and cell wall with plasmodesmata (*arrow*). **d–f** Dying cell from dermal tissue within perforation. **d** Note distorted cell shape, dense staining of nucleus and cytoplasm, cytoplasmic shrinkage and vesicles (*arrow*) within vacuolar area. **e** Nucleus of similar cell. **f** Similar cell showing intact organelles (*arrow*) and separation of cytoplasm from cell wall. **g–i** Dying cell from ground tissue within perforation. **g** Note distorted cell shape, dense staining of nucleus and cytoplasm, vesicles (*arrow*) within the vacuolar area. **h** Similar cell showing misshapen nucleus, intact cell wall and intact organelles. **i** Similar cell showing dense cytoplasm, intact organelles (*arrows*) and cell wall *H*, heterochromatin; *M*, mitochondrion; *N*, nucleus; *O*, nucleolus; *V*, vacuole, *W*, wall *Scale bars* = 2 μ m

multi-nucleolate nuclei and numerous small vacuoles (Fig. 6a, d–f). Numerous mitochondria, proplastids and ribosomes are present in the peripheral cytoplasm, and the thin cell walls are traversed by frequent plasmodesmata (Fig. 6f). By late stage 2, cells adjacent to the perforation site are slightly larger than stage 1 cells, and individual small vacuoles have coalesced to form larger vacuoles (Figs. 6b, c, 7a – c). The large multinucleolate nuclei appear unchanged, but cytoplasm is more diffuse and cell walls are thicker than in stage 1 (compare Fig. 7a with 6 d). In striking contrast, both protoderm and ground meristem cells within the perforation site have misshapen, densely stained nuclei with condensed chromatin (Fig. 7d, e, g, h). The cytoplasm also appears densely stained and collapsed around the nuclei or at the periphery of the cell, although individual organelles

appear to remain intact (Fig. 7f, i). Detached membranes are present in the remnants of the vacuoles (Fig. 7h, i). In most cells, the cytoplasm is retracted from the cell wall and plasmodesmata are visible within the wall, but are disrupted by cytoplasm retraction (Fig. 7h, i). The cell walls are distorted, but appear to remain intact (Fig. 7d–i).

Discussion

Formation of the distinctive perforations in the leaf blades of *Monstera obliqua* is a striking example of developmentally regulated PCD. The death of a discrete subpopulation of cells occurs at a predictable time and place during leaf development. The dying cells display several hallmarks of PCD, including the early degradation of nuclear DNA, as indicated by the presence of TUNEL-positive nuclei and by DNA smearing during gel electrophoresis. Ultrastructural analysis reveals misshapen, densely stained nuclei with condensed chromatin, disrupted vacuoles and condensed cytoplasm. Intact organelles persist until late in the process, and cell walls are distorted, but remain intact. Early expansion of the leaf blade separates the disk of dying cells from adjacent tissue, forming a minute perforation which later extends about 10,000-fold in area as the leaf grows. Perforations arise more or less equidistantly from the earliest-formed lateral veins, and the size variation seen in mature leaves appears to reflect the size of the initial cell population undergoing PCD rather than the timing of perforation formation.

Formation of leaf blade perforations is an extremely rare event across the vascular plants, but also occurs in the submerged aquatic, lace plant, *Aponogeton madagascariensis* (Gunawardena et al. 2004). In the lace plant, perforations also arise at a predictable stage of leaf development and are precisely placed in relation to the completely formed leaf vein system. In both species, DNA degradation as indicated by the TUNEL assay and gel electrophoresis is an early event of PCD, followed by shrinkage and dense staining of the nucleus and cytoplasm and disruption of cellular membranes, although organelles remain intact until late stages. However, the execution of PCD and perforation formation differs between the species in two important respects. First, PCD in lace plant is sequential: it is initiated in a population of cells central to the latent perforation and then a wave of cell death propagates outward from this region until PCD is arrested about five cell layers from the veins (Gunawardena and Dengler 2005). Thus, during early phases of perforation development, a gradient of cells in various stages of PCD exists. This is in striking contrast to *Monstera*, where PCD occurs simultaneously throughout the perforation site and the boundary between dying and healthy cells is sharply delineated. Second, cell wall degradation is an integral part of PCD in the lace plant:

the cell wall matrix appears to be degraded first, followed by cellulose microfibrils. Weakening of the cell walls results in rupture of the leaf blade at each perforation site as the leaf expands. Wall degradation is incomplete in the last cells to die, leaving cell wall remnants at the periphery of the perforation (Gunawardena et al. 2004). We observed no evidence of cell wall degradation in *Monstera*; rather, a desiccated disk of dead tissue with intact cell walls remains attached to the rim of the perforation throughout leaf expansion. It is very likely, however, that a zone of structural weakness is created by a schizogenic-like process during the initial separation between the disk of dying cells and adjacent tissue.

One of the most striking features of perforation formation in *Monstera* is the simultaneous execution of cell death throughout the perforation site. Not only is this unlike perforation formation in lace plant, but also unlike several other well-known examples of developmentally regulated PCD in which cells die progressively. For instance, during the abortion of stamen primordia in the female flowers of maize (*Zea mays*), PCD begins near the apex of the primordium and then spreads basipetally, eventually forming an abrupt border with living cells near the base of the original primordium (Cheng et al. 1983; Calderon-Urrea and Dellaporta 1999). The starchy endosperm tissue of maize and wheat (*Triticum aestivum*) also dies progressively from tip to base during seed development (Young et al. 1997; Young and Gallie, 1999), as does the nucellus of castor (*Ricinus communis*) seeds with the expansion of the endosperm (Greenwood et al. 2005). The progressive development of PCD in these systems suggests that a death signal (or competence to perceive it) might be derived from a unidirectional source or that dying cells might sequentially initiate PCD in their neighbors. In contrast, in *Monstera obliqua* the simultaneous execution of death of the subpopulation of cells at the perforation site suggests that cells perceive and respond to a common death signal in concert. The nature of such a signal in *Monstera* species is completely unknown, but the equidistant placement of perforation sites between the lateral veins suggests that these putative signals could originate in the vascular tissues, much as has been proposed for the placement of specialized cell types in the leaves of many higher plants (Nelson and Dengler 1997).

At the time of initiation of cell death within the perforation sites of *Monstera* leaves, the surrounding tissues are in an active state of cell proliferation and expansion, and mitotic figures are observed in living cells at the boundary of the perforation site. This represents an unusual developmental pattern, in which two cells, previously indistinguishable, have completely different cell fates: one to proliferate and eventually differentiate as an epidermal cell and the other to commit suicide. In many examples of developmentally regulated PCD, whole tissues or organs undergo PCD and, with the exception of stamen abortion in maize (Cheng et al.

1983; Calderon-Urrea and Dellaporta 1999), formation of a sharp boundary across apparently homogeneous, meristematic tissue is rare. Even in the case of tracheary element differentiation in *planta*, complex patterning events such as procambium formation precede PCD in specific cells (Nelson and Dengler 1997). One intriguing possibility for developmentally regulated PCD is that the same trigger might initiate the different signaling pathways that promote either cell proliferation or cell death (Huelskamp and Schnittger 2004). For instance, during the development of the vertebrate limb, a simple limb bud is later re-sculpted by PCD into well-defined domains to form individual digits, a process analogous to perforation formation in *Monstera* and lace plant (Gunawardena et al. 2004; Huelskamp and Schnittger 2004). Bone morphogenetic proteins have been identified as important signals that trigger PCD in the interdigital zones (Merino et al. 1999) and, interestingly, the same molecules have been shown to promote the formation of bones within the digits (Hoffman and Gross 2001). Thus, one signal appears to interact with quite different signaling pathways in cells that are in close proximity.

The occurrence of perforations in the leaf blades of *Monstera* (and other aroid) species and in lace plant represent a striking example of evolutionary convergence. Presumably during the evolutionary origin of leaf perforations in these plants, the signaling pathways and cellular mechanisms of PCD were recruited from other uses of PCD, such as development of tracheary elements or response to pathogens. Although *Monstera* is unlikely to ever be tractable as a system for studying developmentally regulated PCD, it remains a fascinating example of the evolution of novel morphological characters, presumably through placing preexisting PCD pathways under unique spatial and temporal developmental regulation.

Acknowledgements We thank Dr Pauline Wang, Dr Keiko Yoshioka and Danielle Vidaurre for helpful advice on gel electrophoresis and Dr Ron Dengler for photography. We acknowledge funding from the Natural Sciences and Engineering Research Council of Canada for Discovery Grants to NGD and JSG and for a Postdoctoral Fellowship to AHLANG.

References

- Barlow PW (1982) Cell death—an integral part of plant development. In: Jackson MB, Grout B, Mackenzie IA (eds) Growth regulators in plant senescence. Monograph 8, British plant growth regulator group, Wantage, UK, pp 27–45
- Beers EP (1997) Programmed cell death during plant growth and development. *Cell Death Differ* 4:649–661
- Brown VK, Lawton JH (1991) Herbivory and the evolution of leaf shape and size. *Philos Trans Roy Soc Lond B* 333:265–272
- Calderon-Urrea A, Dellaporta S (1999) Cell death and cell protection genes determine the fate of pistils in maize. *Development* 126:435–441
- Cheng PC, Greyson RI, Walden DB (1983) Organ initiation and the development of unisexual flowers in the tassel and ear of *Zea mays*. *Am J Bot* 70:450–462
- Clarke PGH (1990) Developmental cell death—Morphological diversity and multiple mechanisms. *Anat Embryol* 181:195–213
- Dangl JL, Dietrich RA, Thomas H (2000) Cell death and senescence. In: Buchanan B, Gruissem W, Jones RL (eds) Biochemistry and molecular biology of plants. American Society of Plant Physiologists, Rockville, Maryland, pp 1044–1100
- Greenberg JT (1996) Programmed cell death: a way of life for plants. *Proc Natl Acad Sci USA* 93:12094–12097
- Greenwood JS, Helm M, Gietl C (2005) Ricinosomes and endosperm transfer cell structure in programmed cell death of the nucellus during *Ricinus* seed development. *Proc Natl Acad Sci USA* 102:2238–2243
- Groover A, DeWitt N, Heidel A, Jones A (1997) Programmed cell death of plant tracheary elements differentiating in vitro. *Protoplasma* 196:197–211
- Gunawardena AHLAN, Dengler NG (2005) Alternative modes of leaf dissection in monocotyledons. *Bot J Linn Soc* (in press)
- Gunawardena AHLAN, Pearce DM, Jackson MB, Hawes CR, Evans DE (2001a) Characterization of programmed cell death during aerenchyma formation induced by ethylene or hypoxia in roots of maize (*Zea mays* L.) *Planta* 212:205–214
- Gunawardena AHLAN, Pearce DM, Jackson MB, Hawes CR, Evans DE (2001b) Rapid changes in cell wall pectic polysaccharides are closely associated with early stages of aerenchyma formation, a spatially localized form of programmed cell death in roots of maize promoted by ethylene. *Plant Cell Environ* 24:1369–1375
- Gunawardena AHLAN, Greenwood JS, Dengler NG (2004) Programmed cell death remodels lace plant leaf shape during leaf development. *Plant Cell* 16:60–73
- Hoerberichts FA, Woltering EJ (2002) Multiple mediators of plant programmed cell death: interplay of conserved cell death mechanisms and plant-specific regulators. *Bioessays* 25:47–57
- Hoffman A, Gross G (2001) BMP signaling pathways in cartilage and bone formation. *Crit Rev Eukaryot Gene Expr* 11:23–45
- Huelskamp M, Schnittger A (2004) Programmed cell death in development of plant vegetative tissue (leaf and root). In: Gray J (ed) Programmed cell death in plants. Blackwell Publishing, Oxford, UK, pp 106–130
- Ito J, Fukuda H (2002) ZEN1 is a key enzyme in the degradation of nuclear DNA during programmed cell death of tracheary elements. *Plant Cell* 14:3201–3211
- Jones AM (2001) Programmed cell death in development and defense. *Plant Physiol* 125:94–97
- Jones AM, Dangl JL (1996) Logjam at the Styx: Programmed cell death in plants. *Trends Plant Sci* 1:114–119
- Kaplan DR (1984) Alternative modes of organogenesis in higher plants. In: White RA, Dickison WC (eds) Contemporary problems in plant anatomy. Academic, New York, USA, pp 261–300
- Lockshin RA (2004) When cells die. II. A comprehensive evaluation of apoptosis and programmed cell death. Wiley, London
- Madison M (1977) A revision of *Monstera* (Araceae). *Contrib Gray Herb* 207:3–100
- Mayo SJ, Bogner J, Boyce PC (1997) The genera of Araceae. Royal Botanical Gardens, Kew, UK
- Mayo SJ, Bogner J, Boyce PC (1998) Araceae. In: Kubitzki K (ed) The families and genera of vascular plants. IV. Flowering plants—Monocotyledons. Alismatanae and Commelinanae (except Gramineae). Springer Verlag, Berlin, New York, Heidelberg, pp 26–73
- Melville R, Wrigley FA (1969) Fenestration in the leaves of *Monstera* and its bearing on the morphogenesis and colour patterns of leaves. *Bot J Linn Soc* 62:1–16
- Merino R, Ganán Y, Macías D, Rodríguez-León J, Hurlé JM (1999) Bone morphogenetic proteins regulate interdigital cell death in the avian embryo. *Ann NY Acad Sci* 887:120–132
- Morgan PW, Drew MC (2004) Plant cell death and cell differentiation. In: Noodén LD (ed) Plant cell death processes. Elsevier, Amsterdam, pp 19–36

- Nakashima J, Takabe K, Fujita M, Fukuda H (2000) Autolysis during in vitro tracheary element differentiation: formation and location of the perforation. *Plant Cell Physiol* 4:1267–1271
- Nelson T, Dengler N (1997) Leaf vascular pattern formation. *Plant Cell* 9: 1121–1135
- Noodén LD (2004) Introduction. In: Noodén LD (ed) *Plant cell death processes*. Elsevier, Amsterdam, pp 1–18
- Obara K, Fukuda H (2004) Programmed cell death in xylem differentiation. In: Gray J (ed) *Programmed cell death in plants*. Blackwell, Oxford, pp 131–154
- Obara K, Kuriyama H, Fukuda H (2001) Direct evidence of active and rapid nuclear degradation triggered by vacuole rupture during programmed cell death in *Zinnia*. *Plant Physiol* 125:615–626
- Pennell RI, Lamb C (1997) Programmed cell death in plants. *Plant Cell* 9:1157–1168
- Schwartz F (1878) Über die Entstehung der Löcher und Einbuchtungen an dem Blätter von *Philodendron pertusum* Schott. *Sitzber K Akad Wiss Wien Abt I* 77:267–274
- Serguéeff M (1907) Contribution à la morphologie et la biologie des Aponogetonacées PhD dissertation. University of Geneva, Geneva
- Trecul A (1854) Notes sur la formation des perforations que présentent les feuilles de quelques Aroidees. *Ann Sci Nat Bot Biol Veg Ser* 3 20:235–314
- Young TE, Gallie DR (1999) Analysis of programmed cell death in wheat endosperm reveals differences in endosperm development between cereals. *Plant Mol Biol* 39:915–926
- Young TE, Gallie DR, DeMason DA (1997) Ethylene-mediated programmed cell death during maize endosperm development of wild-type and *shrunk2* genotypes. *Plant Physiol* 115:737–751